

**Intermittency of surface-layer wind velocity series in the mesoscale range**

Jean-François Muzy\*

*CNRS UMR 6134, Université de Corse, Quartier Grossetti, 20250 Corte, France*Rachel Baïle<sup>†</sup> and Philippe Poggi<sup>‡</sup>*CNRS UMR 6134, Université de Corse, Vignola, 20200 Ajaccio, France*

(Received 12 December 2009; revised manuscript received 11 March 2010; published 11 May 2010)

We study various time series of surface-layer wind velocity at different locations and provide evidences for the intermittent nature of the wind fluctuations in mesoscale to large-scale range. By means of the magnitude covariance analysis, which is shown to be a more efficient tool to study intermittency than classical scaling analysis, we find that all wind series exhibit similar features than those observed for laboratory turbulence. Our findings suggest the existence of a “universal” cascade mechanism associated with the energy transfer between synoptic motions and turbulent microscales in the atmospheric boundary layer.

DOI: [10.1103/PhysRevE.81.056308](https://doi.org/10.1103/PhysRevE.81.056308)

PACS number(s): 47.27.eb, 47.53.+n, 92.60.Aa, 92.60.Fm

**I. INTRODUCTION**

Atmospheric surface-layer motions are a source of many challenging problems. The issue of designing a faithful statistical model of spatiotemporal wind speed fluctuations has been addressed in various fields such as boundary layer turbulence phenomenology, meteorology, wind power control, and prediction or climatology. From turbulent gusts to hurricanes, breezes to geostrophic wind, the wind process is characterized by a wide range of spatiotemporal scales and all the above mentioned disciplines mainly focus on a specific sub-range of scales. The modeling of wind speed behavior in the mesoscale range is of great interest, for example, in wind power generation or in order to control pollutant dispersion. In this range of scales extending from few minutes to few days ( $\sim 1-1000$  km), the properties of wind velocities are less known than in the range of planetary motions (synoptic scales) or turbulent motions (microscales) [1,2]. From a physical point of view, because of the importance of boundary conditions, the heterogeneous and nonstationary nature of the processes involved, it is well admitted that mesoscale wind regimes strongly depend on various factors such as atmospheric conditions and the nature of the terrain, and may involve periodic variations (caused by diurnal temperature variations). Unlike microscale Kolmogorov homogeneous turbulence, mesoscale fluctuations are therefore not expected to possess any degree of universality [3]. However, during the past few years, some papers have been devoted to the analysis of scaling laws and intermittency features at large scales in many geophysical signals such as temperature, rainfall, or wind speeds [4–6]. In Ref. [3], the authors showed that surface-layer wind velocities recorded at low frequency using a cup anemometer display multiscaling properties very much like in the high-frequency turbulent regime. Moreover, they claimed that random cascade models could be pertinent to reproduce the observed intermittent fluctuations. Along

the same line, in [7], a multifractal detrended analysis was performed on four different hourly wind speed records and revealed some multiscaling properties of the series. Even if these studies did not go beyond simple scaling exponent estimation and did not consider problems related to the statistical significance of the obtained results, they had the merit to address questions about the possible intermittent nature of wind variations in the mesoscale range. As reviewed below, one of the consequences of multiscaling and intermittency is that small-scale fluctuations are strongly non-Gaussian and characterized by “bursty” behavior. In Refs. [8,9], such features have been precisely observed on wind variations statistics at largest microscales (or at smallest mesoscales) and have been shown to be related to a “fluctuating” log-normal turbulent intensity.

In this paper, we suggest that this “fluctuating turbulent intensity” results from a random cascading process initiated at a time scale of few days. Our aim is to show that, in some sense, “turbulent” cascade models are likely to be pertinent at larger scales, in the so-called mesoscale regime. As compared to the previously cited papers, our analysis relies upon the use of magnitude (i.e., logarithms of velocity increments amplitudes) correlation functions. From a mathematical point of view, long-range correlated magnitudes have been shown to be at the heart of the construction of continuous cascade processes [10,11]. For a practical purpose, magnitude covariance possesses interesting properties as far as statistical estimation problems are concerned [12–14]. We show that these correlation functions can be reliably estimated and are very similar to those associated with longitudinal velocity time series of laboratory turbulent experiments. Moreover, we observe some universal features among the various analyzed series.

The paper is organized as follows: in Sec. II, we make a brief review of intermittency and the related notion of random cascade models. We emphasize on the interest of studying magnitude correlations and discuss its relationship with multiscaling properties. We then compare, on an empirical ground, the relative performances of intermittency estimators relying upon scaling and magnitude covariance. This section ends with a review of a recent work of Castaing that has shown how intermittency in Lagrangian and Eulerian frames

\*muzy@univ-corse.fr

†baile@univ-corse.fr

‡poggi@univ-corse.fr

is “observed” on time series recorded at a fixed spatial position. Our main experimental results are then presented in Sec. III. After a rapid description of various wind data we have studied, we show that wind surface-layer variations in mesoscale range have intermittent properties and possess universal magnitude covariance similar to laboratory turbulent fluctuations. Discussions and prospects are reported in Sec. IV.

**II. INTERMITTENCY: FROM MULTISCALING TO MAGNITUDE CORRELATIONS**

**A. Multiscaling and intermittency**

Small-scale intermittency is one of the most challenging problems in contemporary turbulence research. It is generally associated with two distinctive features: the first one is that at small scales the probability density functions (pdf) of velocity variations are strongly leptokurtic (with “stretched exponential” tails) while they are almost Gaussian at larger scales. The second one is that the so-called structure functions display multiscaling properties. As we shall see, these two properties are in fact equivalent within the multiplicative cascade picture. Let us make a brief overview of these notions.

We denote  $X(t)$  a continuous process (for instance, the time variations of a velocity field component at a fixed location) and let  $\delta_\tau X(t)$  be its increments over a scale  $\tau$ :  $\delta_\tau X(t) = X(t+\tau) - X(t)$ . One usually defines the order  $q$  structure function of  $X$  as

$$S_q(\tau) = \int |\delta_\tau X(u)|^q du \tag{1}$$

and the  $\zeta(q)$  spectrum as the scaling exponent of  $S_q(\tau)$ ,

$$S_q(\tau) \underset{\tau \rightarrow 0}{\sim} \tau^{\zeta(q)}. \tag{2}$$

If the function  $\zeta(q)$  is nonlinear one says that  $X(t)$  is a multifractal process or an intermittent process. In that case, as shown, e.g., in [15],  $\zeta(q)$  is necessarily a concave function and the previous scaling holds in the range of small  $\tau$ ,  $\tau \rightarrow 0$  means precisely  $\tau \ll T$ , where  $T$  is a coarse scale called the integral scale in turbulence (in general associated with the injection scale). The intermittency coefficient is a positive number that quantifies the nonlinearity of  $\zeta(q)$  and can be defined<sup>1</sup> as, e.g.,

$$\lambda^2 = -\zeta''(0). \tag{3}$$

The most common example of nonlinear  $\zeta(q)$  function is the so-called *log-normal* spectrum which is a simple parabola,

$$\zeta(q) = \alpha q - \frac{\lambda^2}{2} q^2. \tag{4}$$

In that case  $\lambda^2$  corresponds to the constant curvature of  $\zeta(q)$ .

<sup>1</sup>Notice that one can find different definitions of the “intermittency coefficient” or the “intermittency exponent” in the literature (see [16], for example). However, within the logarithmic-normal cascade model discussed below they are all equivalent.

In order to estimate the multiscaling properties and/or the intermittency coefficient, one can directly estimate partition functions from the data and obtain the exponent  $\zeta(q)$  from a least-squares fit of  $S_q(\tau)$  in log-log representation. However, this method suffers from various drawbacks. First, from a fundamental point of view, one has to distinguish temporal (or spatial) averages from ensemble averages. For instance, in the case of a log-normal multifractal, rigorously speaking, only the “ensemble” average  $\langle |\delta_\tau X(u)|^q \rangle$  behaves as a power law with an exponent  $\zeta(q)$  as given by Eq. (4). The temporal or spatial average has an exponent spectrum  $\zeta(q)$  that becomes linear above some value of  $q$  and is no longer parabolic [17]. In order to estimate  $\zeta(q)$  from moment scaling over a wide range of  $q$  one has to use the so-called “mixed” asymptotic framework [18]. But the main problem remains that high-order moment estimates require very large sample size. Moreover, the scaling behavior can also be altered by finite-size effects, discreteness, and nonstationarity effects such as periodic perturbations or periodic modulations of the data (see below). A more reliable method first introduced in [12] (see also [19]) relies upon the so-called magnitude cumulant analysis. It simply consists of focusing on the scaling behavior of partition functions around  $q=0$ . According to this approach, the structure function is written as

$$S_q(\tau) = \exp \left[ \sum_{k=1}^{\infty} C_k(\tau) \frac{q^k}{k!} \right], \tag{5}$$

where  $C_k(\tau)$  is the  $k$ th cumulant associated with the random variable  $\omega_\tau(u) = \ln(|\delta_\tau X(u)|)$ . The logarithm of the increment will henceforth be referred to as the *magnitude* of velocity increments. Note that  $C_1$  is simply the mean value of  $\omega$  while  $C_2$  is its variance. Thanks to the scaling relationship Eq. (2), one deduces that all cumulants behave as

$$C_k(\tau) = c_k \ln(\tau) + r_k, \tag{6}$$

where the constants  $\{r_k\}$  account for both the integral scale and the prefactors in the scaling relationship Eq. (2). The function  $\zeta(q)$  can therefore be expressed in terms of a cumulant expansion,

$$\zeta(q) = \sum_k c_k \frac{q^k}{k!}. \tag{7}$$

In particular one sees that the intermittency coefficient is directly involved in the behavior of the magnitude variance as

$$C_2(\tau) = -\lambda^2 \ln(\tau) + r_2. \tag{8}$$

Equation (8) has been successfully used to estimate the intermittency coefficient of longitudinal velocity fields in three-dimensional (3D) fully developed regime under various experimental conditions. A common value close to  $\lambda^2 \approx 0.025$  has been obtained. It is remarkable that this intermittency value appears to be universal [12,19,20].

Let us end this brief review by discussing the relationship between intermittency and the small-scale bursty behavior of velocity increments. Indeed, it is well known in turbulence laboratory experiments that large-scale increment pdf’s are close to being normal while small scales have larger tails.

The flatness strongly increases when one goes from large to small scales. We focus only on the log-normal case, i.e., a parabolic  $\zeta(q)$ , extension of our considerations to other laws being straightforward. Thanks to the structure function multiscaling interpreted as a moment equality, by simply performing a time scale contraction,  $\tau' = s\tau$  ( $s < 1$ ), one can write

$$\delta_{s\tau} X = e^{\Omega_s} \delta_\tau X, \quad (9)$$

Law

where  $\Omega_s$  is a Gaussian random variable of variance  $-\lambda^2 \ln(s)$  which law is denoted as  $G_s(\Omega)$ . By simply assuming that for  $\tau = T$  ( $T$  being the integral scale), the increments of  $X$  are normally distributed, one obtains the small-scale pdf of  $\delta_\tau X$  by the well known Castaing formula [21],

$$p(z, \tau) = (2\pi)^{-1/2} \int G_{\tau/T}(\Omega) e^{\Omega} e^{-e^{-2} \Omega^2 / 2} d\Omega. \quad (10)$$

This means that, at scale  $\tau$ , the pdf's of the increments of the process  $X(t)$  are obtained as a superposition of Gaussian distributions of variance  $e^{2\Omega}$ , where  $\Omega$  is itself a Gaussian random variable of variance increasing at small scales like  $\lambda^2 \ln(T/\tau)$ . The smaller the scale, the larger the variance of  $\Omega$  and therefore the larger the tails of the increment pdf  $p(z, \tau)$ . The continuous deformation from Gaussian at large scales toward stretched exponential like shapes at small scales, observed in laboratory turbulence experiments, has been shown to be well accounted by the transformation (10).

### B. Random cascades and logarithmic magnitude covariance

A natural question that arises after the previous analysis is how can we explicitly build models that possess multiscaling properties? In other words, since multiscaling is equivalent to intermittency, how can the variance of the magnitude increase as a logarithm of the scale as described by Eq. (8)? The answer comes from the self-similarity Eq. (9) that can be iterated and interpreted as a random cascade: when one goes from large to small scales, one multiplies the process by a random variable  $W_s = \exp(\Omega_s)$ .

Usually one starts by building a nondecreasing (i.e., with positive variations) cascade process, denoted hereafter as  $M(t)$ , which is often referred to as a multifractal *measure* though its variations are not bounded. More general multifractal processes (or multifractal “walks”) can be simply obtained by considering a simple Brownian motion  $B(t)$  (or any self-similar random process) compounded with the measure  $M(t)$  considered as a stochastic time:  $X(t) = B[M(t)]$ . In the finance literature  $M(t)$  is often referred to as the “trading time” while in turbulence  $M(t)$  can be associated with the spatial or temporal distribution of energy dissipation. The statistical properties of  $X(t)$  can be directly deduced from those of  $M(t)$  (see, e.g., [22,23]). Random multiplicative cascades measures were originally introduced as models of the energy cascade in fully developed turbulence. After the early works of Mandelbrot [24–26], a lot of mathematical studies have been devoted to discrete random cascades [27–31]. Let us summarize the main properties of these constructions, set

some notations and see how these notions extend to continuous cascades.

The simplest multifractal discrete cascades are the dyadic cascades defined by the following iterative rule: one starts with some interval of constant density and splits this interval in two equal parts. The density of the two subintervals is obtained by multiplying the original density by two (positive) independent random factors  $W$  of same law. This operation is then repeated *ad infinitum*. The integral scale corresponds to the size of the starting interval. A log-normal cascade corresponds to  $W = \exp(\Omega)$  where  $\Omega$  is normally distributed. Peyrière and Kahane [27] proved that this construction converges almost surely toward a stochastic nondecreasing process  $M_\infty$  provided  $\langle W \ln W \rangle < 1$ . The multifractality of  $M_\infty$  (hereafter simply denoted as  $M$ ) and of  $X(t) = B(M(t))$  [ $B(t)$  being a Brownian motion] has been studied by many authors (see, e.g., [29]) and it is straightforward to show that the spectrum of  $X(t)$  is

$$\zeta(q) = q/2 - \ln_2 \langle W^{q/2} \rangle. \quad (11)$$

The self-similarity Eq. (9) for dilation factors  $s = 2^n$  can also be directly deduced from the construction.

Because the discrete cascade construction involves dyadic intervals and a “top-bottom” construction it is far from being stationary. In order to get rid of these drawbacks, continuous cascade constructions have been recently proposed and studied on a mathematical ground [11,22,23,32–34]. They share exact multifractal scaling with discrete cascades but they display continuous scaling and possess stationary increments [11,22,23,33]. Without entering into details, we just want to stress that these constructions rely upon a family of infinitely divisible random processes  $\Omega_l(t)$ . The process  $M(t)$  is obtained as the weak limit, when  $l \rightarrow 0$ , of  $\int_0^t e^{\Omega_l(v)} dv$ . In the log-normal case,  $\Omega_l$  is simply a Gaussian process defined by a covariance function that mimics the behavior of discrete cascade. In Refs. [10,35] it has been shown that such a correlation function decreases slowly as a logarithm function,

$$\begin{aligned} \rho(\Delta t) &\stackrel{\text{def}}{=} \text{cov}[\Omega_l(u), \Omega_l(u + \Delta t)] \\ &\simeq -\lambda^2 \ln \left( \frac{\Delta t + l}{T} \right) \quad \text{for lags } \Delta t \leq T. \end{aligned} \quad (12)$$

The integral scale  $T$  where cascading process “starts” can therefore be interpreted as a *correlation length* for the variation logarithmic amplitudes of  $X(t)$ . Notice that the regularization for  $\Delta t \leq l$ , represented by the offset  $l$ , can be slightly modified without changing the final results [23]. The so-called multifractal random walk (MRW) process introduced in Ref. [11] consists of constructing a log-normal multifractal process  $X(t) = B[M(t)]$  where  $B(t)$  is a Brownian motion and

$$M(t) = \lim_{l \rightarrow 0^+} \int_0^t e^{\Omega_l(u)} du, \quad (13)$$

where  $\Omega_l(u)$  is a Gaussian process with a logarithmic covariance as given in Eq. (12). In Figs. 1(a) and 1(b) are plotted, respectively, a sample of a log-normal measure  $M(dt)$  ( $dt = 1$ ) and a path of a MRW process  $X(t)$  corresponding to  $\lambda^2 = 0.025$  and  $T = 512$ .

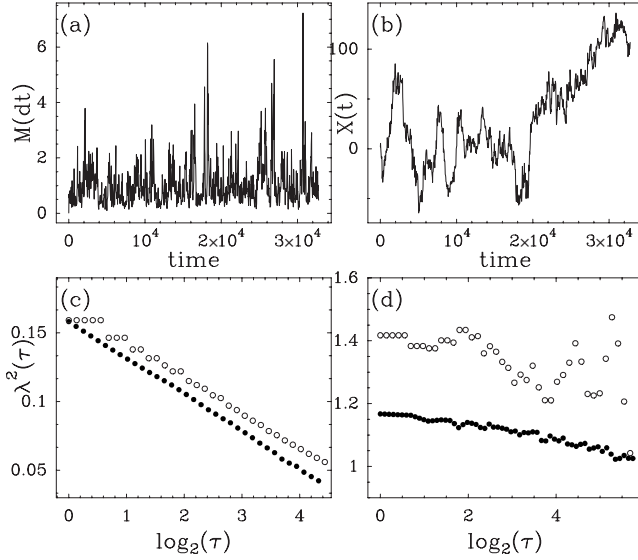


FIG. 1. Estimation of the intermittency coefficient for (a) a log-normal MRW multifractal measure and (b) a log-normal MRW process. In both cases the sample size is 32 768 points,  $\lambda^2=0.025$ , and  $T=512$ . In (c) are plotted the magnitude covariance (●) and magnitude variance (○) as a function, respectively, of the logarithm of the lag and the logarithm of the scale. The slope of both curves provides an estimation of  $\lambda^2$ . One can see that for measure  $M(dt)$ , the errors in the estimation are comparable. In (d) are displayed the same plots as in (c) but for the magnitude of the MRW process. Because of the additive noise and the small number of independent points at large scales, the estimation relying upon the magnitude variance turns out to be much more altered.

The studies devoted to continuous versions of discrete cascades have mainly shown that multifractal processes are related to exponential or logarithmic correlated random processes. The magnitude covariance function has been proven to be at the heart of the notion of “continuous cascade.” As we shall see below, it also allows one to estimate the intermittency coefficient in a more reliable way than methods based on scaling properties.

### C. Intermittency coefficient estimation issues

As far as the problem of the intermittency coefficient estimation is concerned, it results from previous discussion that this coefficient, originally defined as the curvature of  $\zeta(q)$ , can be estimated either from the behavior of magnitude variance across scales [Eq. (8)] or from the slope of the time magnitude covariance in lin-log coordinates [Eq. (12)]. In fact, the two methods we would like to compare rely upon two different interpretations of the self-similarity Eq. (9). Indeed, for a continuous cascade (MRW) process  $X(t)$ , this equation can be shown to be an equality in law for all finite dimensional distributions (f.d.d.). By taking the logarithm, one gets

$$\omega_\tau(u) = \ln(|\delta_\tau X(u)|) \underset{f.d.d.}{=} \Omega_\tau(u) + \ln(|\varepsilon(u)|), \quad (14)$$

where  $\Omega_\tau(u)$  is a logarithmic-correlated Gaussian random variable [Eq. (12)], which variance behaves like in Eq. (8)

while  $\varepsilon(u)$  is a standardized normal white noise independent of  $\Omega_\tau$ . All “scaling” methods [such as Eq. (8) or (10)] consist of interpreting the previous equality at a given fixed location  $u$  for various scales  $\tau$ . Since  $\varepsilon$  does not depend on  $\tau$ ,  $\lambda^2$  is estimated by a linear regression of  $\text{var}(\omega_\tau)$  as a function of  $\ln(\tau)$ . Alternatively, the method relying on Eq. (12) consists of exploiting the temporal dependence of Eq. (14) at a fixed  $\tau$  value. Since  $\ln(|\varepsilon|)$  is a white noise,  $\lambda^2$  can be obtained as the slope of the estimated covariance of  $\omega_\tau$  as a function of the logarithm of the lag  $\ln(\Delta u)$ . Let us discuss why magnitude covariance based estimation (hereafter referred to as *method II*) is much more reliable than scaling magnitude cumulant analysis (referred to as *method I*) in the case of multifractal random walks.

The precise computation of the properties of these estimators is a difficult task so we only aim at obtaining a rough estimate of the relative performance of each method. In Ref. [36], it has been shown that a generalized method of moments relying on the magnitude correlation function provides an unbiased and consistent estimator of  $\lambda^2$ . Estimators relying on Eq. (8) have been precisely discussed within the context of atmospheric turbulence in Ref. [19] where the authors showed that it allowed one, by means of a bootstrap method called “surrogate analysis,” to estimate  $\lambda^2$  and distinguish intermittent from non-intermittent time series.

If one denotes by  $\mathcal{E}_I$  and  $\mathcal{E}_{II}$  the estimation error of  $\lambda^2$  associated with, respectively, methods I and II, we show in the Appendix that

$$\mathcal{E}_I^2 \approx \frac{2T\lambda^4}{N} + \frac{16T}{N(\ln T)^3}, \quad (15)$$

$$\mathcal{E}_{II}^2 \approx \frac{2T\lambda^4}{N} + \frac{1}{N(\ln T)^3}, \quad (16)$$

where  $N$  is the overall sample size,  $T$  is the integral scale, and  $\lambda^2$  is the intermittency coefficient. The two terms in the r.h.s are the estimation errors associated with, respectively,  $\Omega_\tau(u)$  and the “noise”  $\ln(|\varepsilon(u)|)$  in Eq. (14). The difference between the two methods is clearly caused by the presence of the noise term. As illustrated in Fig. 1(c) where both estimators are computed from a sample of a log-normal multifractal random measure  $M$  [Fig. 1(a)], when one has directly access to  $\Omega_\tau$  ( $\Omega_\tau(u) = \ln M([u, u + \tau])$ ), both estimators (methods I and II) are roughly equivalent. This is obviously not the case in the presence of the noise term in Eq. (14), i.e., when one studies the increments of a MRW process  $X(t)$  [Fig. 1(d)]. It can be seen in Eqs. (15) and (16) that the error associated with  $\ln(\varepsilon)$  is greater in the case of method I. The two methods will have errors of the same magnitude order only when

$$\lambda^4 \geq \frac{8}{(\ln T)^3}. \quad (17)$$

For a typical integral scale value  $\ln T \approx 6$  (see below) this gives  $\lambda^2 \geq 0.2$ . Consequently, when  $\lambda^2 \leq 0.2$ , the method relying on the estimated covariance provides better results than the estimation from the scaling of the variance. Let us define the ratio between the errors of the two methods as

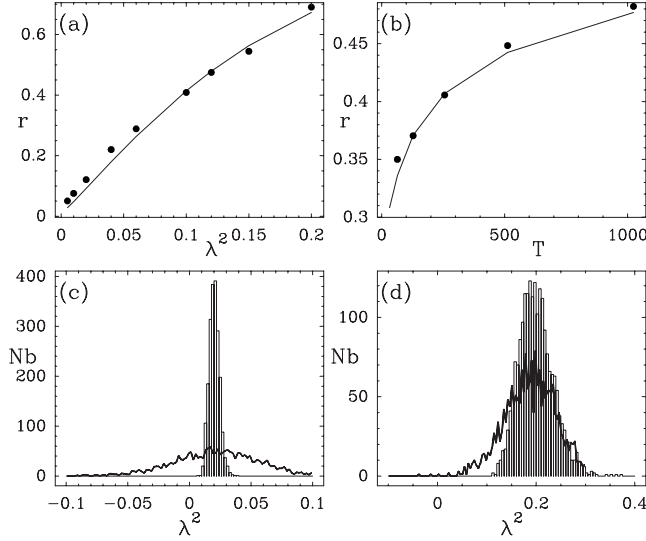


FIG. 2. Comparison of the two estimation methods of the intermittency coefficient for a log-normal MRW process (a) Error ratio  $r = \mathcal{E}_{II} / \mathcal{E}_I$  as a function of  $\lambda^2$  for  $T=256$  and  $N=8192$ . (b) Error ratio  $r = \mathcal{E}_{II} / \mathcal{E}_I$  as a function of  $T$  for  $\lambda^2=0.03$  and  $N=8192$ . In (a) and (b) the errors have been estimated using 2048 Monte Carlo samples. Symbols (●) represent the observed error ratios while the solid line stand for the analytical expressions derived from Eqs. (15) and (16). (c) Histograms of estimated values of  $\lambda^2$  using method I (solid line) and method II (bars) for  $\lambda^2=0.02$ ,  $T=512$ , and  $N=8192$ . (d) Same plots as in (c) for  $\lambda^2=0.2$ .

$$r = \frac{\mathcal{E}_{II}}{\mathcal{E}_I}. \quad (18)$$

This expression can be computed as a function of  $T$  and  $\lambda^2$ . In Figs. 2(a) and 2(b) we have plotted the value of  $r$  as a function of  $\lambda^2$  for a fixed value  $T=256$  and as a function of  $T$  for  $\lambda^2=0.03$ , respectively. We see that the observed ratio  $r$  is an increasing function of  $\lambda^2$  and  $T$  rather close to the prediction we get from expressions (15) and (16). For  $\lambda^2=0.02$ , a typical value observed in many applications, we have  $r \leq 0.1$ , i.e., method I has an error more than ten times greater than method II. This is confirmed Fig. 2(c) where we have reported the histogram of the estimated  $\lambda^2$  with both methods over 2048 experiments. The histogram obtained with method II is sharply peaked around the expected value, while the estimates of method I are spread over a large interval. For greater  $\lambda^2$ , one sees in Fig. 2(d) that the two histograms have comparable widths ( $\lambda^2=0.2$ ).

#### D. Squared logarithmic magnitude covariance as the result of Lagrangian and Eulerian intermittency

In most fluid mechanics experiments, one usually records one or several components of the velocity field using an anemometer, so one has only access to the values of the field at a fixed spatial position as a function of time. In order to make inferences on the spatial properties of the velocity, i.e., the Eulerian field, one generally invokes the Taylor frozen hypothesis or, when the turbulence rate is large, the Tenekes sweeping argument according to which small-scale velocity

fluctuations are mainly caused by Eulerian variations advected by large-scale random motions [37]. However, as explained below, for some functions, single point measurements cannot be linked so easily to their Eulerian counterpart. Hereafter, we reproduce the argument of Castaing [38,39] in order to understand the shape of the single point magnitude covariance if one supposes that both Eulerian and Lagrangian velocity fluctuations are given by a continuous cascade as described previously.

Let us denote  $\Omega(x, t)$  the magnitude at time  $t$  and position  $x$ . It is important to notice that  $\Omega(x, t)$  is a local field that does not depend on any spatial or time scale (for example in turbulence,  $\Omega(x, t)$  can be considered as the logarithm of the dissipation field or of the velocity increments at a scale smaller than the Kolmogorov dissipation scale). Our goal is to compute

$$\text{cov}[\Omega(x, t), \Omega(x, t + \Delta t)], \quad (19)$$

as a function of the time lag  $\Delta t$  for a fixed value of  $x$ .

If one supposes that both Eulerian and Lagrangian fields  $\Omega$  are logarithmic correlated, i.e., well described by a continuous cascade model, then

$$\text{cov}[\Omega(x, t), \Omega(x + r, t)] = \lambda^2 \ln\left(\frac{L}{r + \eta_e}\right),$$

$$\text{cov}[\Omega(x(t), t), \Omega(x(t + \Delta t), t + \Delta t)] = \mu^2 \ln\left(\frac{T}{\Delta t + \eta_l}\right),$$

where  $\Delta t$  and  $r$  are time and space lags,  $\eta_e$  and  $\eta_l$  are small-scale spatial and temporal cutoffs (i.e., the Kolmogorov scales in turbulence),  $L$  and  $T$  are spatial and temporal integral scales and  $\lambda^2$ ,  $\mu^2$  are Eulerian and Lagrangian intermittency coefficients.

Let us suppose that the fluid particle at position  $x$  at time  $t + \Delta t$  was at position  $x'$  at time  $t$ . Thanks to the above covariance formula, one can write,

$$\Omega(x, t + \Delta t) = \rho_1 \Omega(x', t) + \epsilon, \quad (20)$$

where  $\epsilon$  is a random variable independent of  $\Omega(x', t)$  and

$$\rho_1 = \frac{\mu^2 \ln\left(\frac{T}{\Delta t + \eta_l}\right)}{\text{var}(\Omega)}. \quad (21)$$

But (at least from a statistical point of view)  $r = |x' - x| = V\Delta t$ , where  $V$  is a ‘‘typical’’ velocity (the mean or rms velocity) so that, if one assumes that  $L \approx VT$ ,

$$\Omega(x', t) = \rho_2 \Omega(x, t) + \epsilon', \quad (22)$$

where  $\epsilon'$  is a random variable independent of  $\Omega(x, t)$  and

$$\rho_2 = \frac{\lambda^2 \ln\left(\frac{VT}{V\Delta t + \eta_e}\right)}{\text{var}(\Omega)}. \quad (23)$$

Then, if  $\epsilon$  and  $\epsilon'$  are uncorrelated, since the correlation coefficient between  $\Omega(x, t)$  and  $\Omega(x, t + \Delta t)$  is the product  $\rho_1 \rho_2$ , we have

TABLE I. Main features of the time series.

Location	Latitude	Longitude	Dates	Sampling freq.	Site
Vignola (Ajaccio)	41°56'N	8°54'E	1998–2003	1 min	50 m, coastal, high hills
Ajaccio	41°55'N	8°47'E	2002–2006	1 h	5 m, coastal, plain, airport
Bastia	42°33'N	9°29'E	2002–2006	1 h	10 m, coastal, plain, airport
Calvi	42°31'N	8°47'E	2002–2006	1 h	57 m, coastal, hills
Conca	41°44'N	9°20'E	2002–2006	1 h	225 m, high hills
Figari	41°30'N	9°06'E	2002–2006	1 h	21 m, plain, airport, hills
Renno	42°11'N	8°48'E	2002–2006	1 h	755 m, mountains
Sampolo	41°56'N	9°07'E	2002–2006	1 h	850 m, mountains
Eindhoven	51°44'N	5°41'E	1960–1999	1 h	20 m, plain
I. J. Muiden	52°46'N	4°55'E	1956–2001	1 h	4 m, coastal, plain
Schiphol	52°33'N	4°74'E	1951–2001	1 h	–4 m, plain, airport

$$\text{cov}[\Omega(x,t), \Omega(x,t + \Delta t)] = \text{var}(\Omega)\rho_1\rho_2, \quad (24)$$

and by taking into account the fact that  $\text{var}(\Omega) = \mu^2 \ln(T/\eta_l) = \lambda^2 \ln(L/\eta_e)$  one obtains finally, to the first order, in the limit of lags  $\Delta t$  such that  $V\Delta t \gg \eta_e$  and  $\Delta t \gg \eta_l$ ,

$$\text{cov}[\Omega(x,t), \Omega(x,t + \Delta t)] = \frac{\lambda^2}{\ln\left(\frac{T}{\eta_l}\right)} \ln^2\left(\frac{\Delta t}{T}\right) \left\{ 1 + O\left[\frac{\eta^*}{\Delta t \ln\left(\frac{T}{\Delta t}\right)}\right] \right\} \quad (25)$$

$$= \frac{\mu^2}{\ln\left(\frac{L}{\eta_e}\right)} \ln^2\left(\frac{\Delta t}{T}\right) \left\{ 1 + O\left[\frac{\eta^*}{\Delta t \ln\left(\frac{T}{\Delta t}\right)}\right] \right\}, \quad (26)$$

where  $\eta^* = \max(\eta_l, V^{-1}\eta_e)$ .

By representing  $\sqrt{\text{cov}}$  as a function of  $\ln(\tau)$ , if one neglects the small corrections  $O(\eta^*/[\Delta t \ln(T/\Delta t)])$ , one expects a straight line of slope,

$$r = \sqrt{\frac{\lambda^2}{\ln\frac{T}{\eta_l}}} = \sqrt{\frac{\mu^2}{\ln\frac{L}{\eta_e}}}. \quad (27)$$

If one knows the ‘‘Reynolds numbers’’  $L/\eta_e$  and  $T/\eta_l$ , the intermittency coefficients can be estimated from the slope  $r$  as,

$$\lambda^2 = r^2 \ln\left(\frac{T}{\eta_l}\right), \quad (28)$$

$$\mu^2 = r^2 \ln\left(\frac{L}{\eta_e}\right). \quad (29)$$

We see that, by taking into account both Eulerian and Lagrangian fluctuations on single point measurements, one should observe a squared logarithm magnitude covariance instead of the logarithmic behavior of Eq. (12). This peculiar shape of magnitude covariance has indeed been precisely observed on laboratory fully developed turbulence data in Ref. [12].

### III. RESULTS: INTERMITTENCY IN MESOSCALE WIND FLUCTUATIONS

#### A. Data series

The results reported in the following are based on different wind velocity time series. The first data set consists of horizontal wind speeds and directions that have been recorded every minute during 5 years (1998–2002) at our laboratory in Ajaccio-Vignola at a height of 10 m by means of a cup anemometer. We also study hourly wind speed and direction data (10 min averages) for seven different sites in Corsica (France). The length of these series is also 5 years. These data have been measured and collected by the French Meteorological Service of Climatology (Meteo-France) using a cup anemometer and wind vane at 10 m above ground level. Finally, we also consider potential winds from KNMI HYDRA PROJECT available online [40]: they represent series of hourly (1 h average), 10 m potential wind speed gathered during several years at various locations in Netherlands. More specifically we consider the series recorded at three different sites over a long period of several decades. Table I summarizes the main characteristics of the studied series.

In the sequel,  $v(t)$  will denote the modulus of the velocity horizontal vector while  $v_x(t)$  and  $v_y(t)$  will stand for its two components along arbitrary orthogonal axes  $x$  and  $y$ . We have by definition,

$$v(t) = \sqrt{v_x(t)^2 + v_y(t)^2}.$$

Because there is no well defined constant mean velocity direction with a small turbulent rate, we have chosen to study  $v_x$  and  $v_y$  separately instead of considering meaningless longitudinal and transverse components.

The power spectrum analysis is one of the most common tools for analyzing random functions and is at the heart of a wide number of studies of wind velocity statistics. Since the pioneering work of Van Der Hoven [41,42], the shape of a typical atmospheric wind speed spectrum in the atmospheric boundary layer is still matter of debate. It is relatively well admitted that it possesses two regimes separated by low energy valley called the ‘‘spectral gap’’ located at frequencies around few minutes. This gap separates the microscale re-

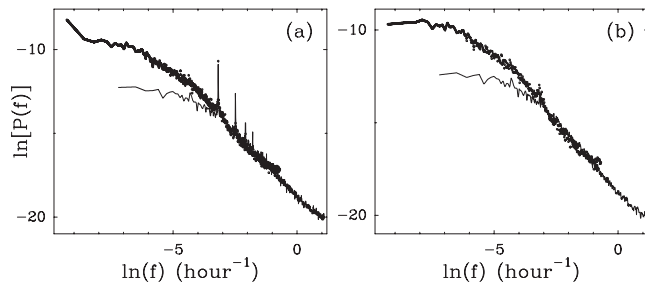


FIG. 3. Power spectrum density of  $v_x$  wind components 10 min rate Vignola series (solid line) and hourly Eindhoven series (dotted line) in log-log representation. (a) One clearly identifies the peaks associated with diurnal oscillation superimposed to an overall scaling regime where  $P(f) \sim f^{-\beta}$  with  $\beta \approx 1.6$ . This regime roughly extends from few days to few minutes. (b) Plot of the same spectra where the estimated additive local seasonal components have been removed.

gime, where turbulent motions take place, from the mesoscale range. In the homogeneous turbulent regime, it is well known that the spectrum associated with the velocity field behaves like  $E(k) \sim k^{-5/3}$  as predicted by Kolmogorov in 1941 [1] ( $k$  is the spatial wave number). In the mesoscale range, for time scales greater than few minutes, the shape of this spectrum appears to depend on various factors. If some experiments suggest that a  $k^{-5/3}$  spectrum can extend up to synoptic scales [43,44] in the free atmosphere, things are different in the surface layer [45]. Some authors suggest that statistics *a priori* depend on local conditions (orographic, atmospheric, etc.) and one does not expect the same degree of universality as in the microscale regime (let us mention that, as far as turbulence is concerned, it is commonly known that some quantities such as the mean velocity value or the turbulent rate are strongly dependent on local conditions). For example, in Ref. [3], it is shown that the spectrum exponent may depend on the atmospheric stability conditions and also on the topography.

In Fig. 3 are plotted the power spectrum of the  $v_x$  component of two series: the “high-frequency” (10 min rate) series of Vignola and the hourly series recorded at Eindhoven. These two spectra, which do not cover the same energy range, have been shifted by an arbitrary multiplicative factor in the  $y$  direction in order to have comparable values. Series associated with the  $v_y$  component or corresponding to other sites have similar features. One can see that, up to the main peaks associated with diurnal wind oscillations (see below), these spectra are well described by a power law  $P(f) \sim f^{-\beta}$  in a frequency domain which corresponds to time scales from few minutes to a characteristic time of few days (note that the low-frequency behavior is much more reliable in the Eindhoven series since it covers a period close to ten times longer than the Vignola series). The value of the exponent is  $\beta \approx 1.6$  for both sites. Within the framework of self-similar Gaussian processes [46], the fact that  $\beta > 1$  for all series indicates that the signal process  $v_x(t)$  has continuous paths. Since at low frequency the spectrum becomes flat, this means that the process appears regular at small scales and more “noisy” at larger scales. This feature is illustrated in Fig. 4 where we have plotted two samples of the component

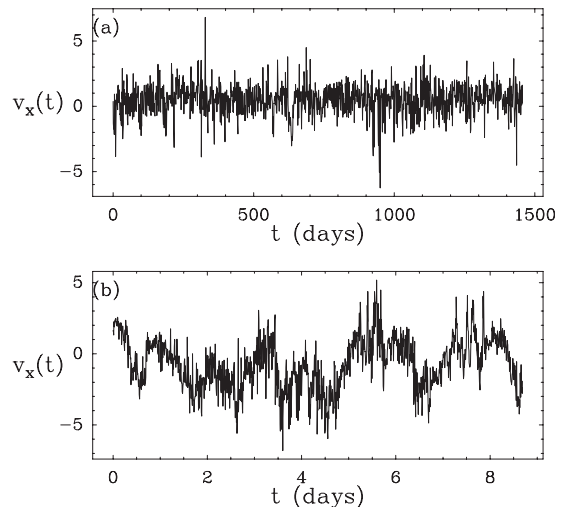


FIG. 4. Time fluctuations of the  $v_x(t)$  component of the Vignola velocity field (original data). (a) At large time scales, one does not see any structure; we are in the flat (white noise) regime of the power spectrum. (b) At a finer time resolution, the series appears as a superposition of turbulent gusts and a more regular component.

$v_x(t)$  of Vignola wind series over two different time intervals. At very large scale, the signal looks like a highly irregular “white noise” that corresponds to the power-spectrum low-frequency flat behavior [Fig. 4(a)] while a zoom over a finer time interval reveals more regular variations [Fig. 4(b)]. Notice that one can also observe a daily oscillating behavior and high-frequency turbulent gusts superimposed to these regular random variations.

Since our goal is to study the stationary random components of the velocity field, we have preprocessed all time series in order to remove the additive seasonal components. In fact the diurnal oscillations  $S_{x,y}$  are not really periodic but vary during the year according to the sun position. We have used a local harmonic parametrization of these components and computed the parameters by minimizing an exponential moving average of a quadratic error (see [47,48] for more details). In order to study the fluctuations in these deseasonalized series and an eventual intermittency, we can compute, as in the turbulence literature, its increments. Notice that one can alternatively study velocity component wavelet coefficients or, if one wants to account for the low-frequency behavior, the error in the one step forward prediction of a Langevin like modeling of  $v_x(t)$  and  $v_y(t)$  [48],

$$v_{x,y}(t+1) = S_{x,y}(t+1) + (1 - \gamma)[v_{x,y}(t) - S_{x,y}(t)] + w_{x,y}(t), \quad (30)$$

where the friction coefficient  $\gamma$  is estimated to be  $\gamma \approx 1 \text{ day}^{-1}$ ,  $S_{x,y}(t)$  stands for the seasonal additive component of the wind velocity, and  $w_{x,y}(t)$  is the error (noise) term. Whatever is the precise definition used to compute the local fluctuations, the results presented in the next section remain unchanged.

## B. Evidences for a mesoscale cascade

As recalled in the Introduction, unlike inertial subrange turbulence, few papers have been devoted to the study of

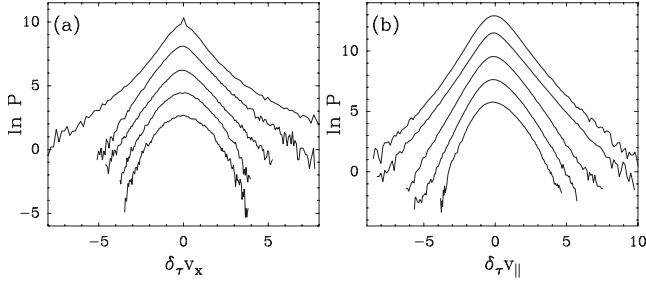


FIG. 5. Semilogarithmic representation of standardized velocity increment pdf at various scales. From top to bottom one goes from small to coarse time scales. All graphs have been vertically shifted for the sake of clarity. (a) Logarithm of the pdf of the deseasonalized wind velocity increments  $\delta_\tau v_x$  for the Eindhoven wind series. Time scales  $\tau$  go from 1 h to 5 days. (b) Same plots as in (a) but for the increments of the longitudinal velocity field  $\delta_\tau v_{\parallel}$  in a high Reynolds number turbulence experiment (see text). Scales  $\tau$  extend from the Kolmogorov scale to the integral scale.

scaling properties of atmospheric fields from moderate to large scales. In Ref. [4], the authors found that cloud satellite data display multiscaling over the range  $1-5 \times 10^3$  km and suggest the existence of a (anisotropic) cascade process from planetary scales down to the microscales. As far as scaling properties of surface-layer wind speed are concerned, some studies focus on (multi)scaling properties. In Ref. [7], the authors used detrended fluctuation analysis on various hourly averaged wind series and provided evidences of a crossover between two scaling regimes separating mesoscale range from very-large-scale range. The scale of the crossover was found to be  $T \approx 5$  days and the author conjectured the possibility of the existence of multiscaling for scales below this scale. In that case the scale  $T$  could be identified to some integral (injection) scale. In Refs. [3,49], Lauren *et al.* performed an analysis and a modeling of atmospheric wind in both mesoscale and microscale (turbulent) regimes. They showed that the concepts of multiscaling and cascades are also pertinent for characterizing and simulating low-wave numbers properties of surface-layer winds.

Although the above mentioned studies provide hints for the existence of intermittency in wind fluctuations at large scales, as explained in Sec. II, because of diurnal oscillations, discreteness of the data, limited size of the scaling range, and for purely statistical considerations, the reported estimations of (multi)scaling properties of mesoscale wind data are far from being reliable. A more direct and convincing illustration of the intermittent nature of mesoscale wind variations is provided in Fig. 5(a) where we have plotted the normalized pdf of the increments of (deseasonalized) wind components  $v_x$  of the Eindhoven site in logarithmic scale. One sees that increment distributions go from “stretched exponential” like functions (with large tails) to Gaussian-like behavior (parabola) when going from 1 h to few days time scales. This behavior is very similar to the features observed in fully developed turbulence laboratory experiments. In Fig. 5(b), for comparison purpose, we have plotted in the same logarithmic scale the standardized pdf of longitudinal velocity increments computed from experimental data obtained by Chabaud and Castaing in a low-temperature gaseous helium

jet experiment [50] (the Taylor scale based Reynolds number is  $R_\lambda = 929$ ). As the scale  $\tau$  varies from the dissipation to the integral scale, one observes the same deformation of the pdf from large tailed shape to Gaussian-like shape. As explained in Sec. II A [Eq. (10)], such a variation of the pdf behavior across scales is usually associated with the existence of an intermittent cascade. Let us notice that the smallest time scales we considered correspond to scales greater than or equal to the “injection” largest scale of atmospheric boundary layer turbulence. Consequently, according to our observations, velocity increment statistics at large (atmospheric surface-layer) turbulent scales are characterized by a strong kurtosis. This contrasts with the situation in laboratory experiments where the distribution are nearly Gaussian at large scales [as illustrated by the bottom graph in Fig. 5(b)]. Similar observations have been performed in [8,9]. In [8], the authors interpret the intermittency of large-scale atmospheric turbulence by the fluctuations of the turbulence intensity at this scale. The velocity mean is no longer constant but stochastic. Similar observations on the vorticity field have been made in [9]. In the following, we suggest that these fluctuations of turbulence intensity can be interpreted as the result of a cascading process starting at a larger time scale.

As advocated in Sec. II C, the best way to reveal the presence of an underlying random cascade and to estimate the intermittency coefficient is to study the magnitude correlations functions associated with velocity small-scale variations. If one writes Eq. (14) for the small-scale increments of, respectively,  $v_x$  and  $v_y$  (where the seasonal components have been removed) one can define two magnitude processes and two processes  $\Omega_x$  and  $\Omega_y$ :

$$\omega_{x,\tau}(t) \equiv \ln(|\delta_\tau v_x(t)|) = \Omega_{x,\tau}(t) + \ln(|\epsilon_x(t)|),$$

$$\omega_{y,\tau}(t) \equiv \ln(|\delta_\tau v_y(t)|) = \Omega_{y,\tau}(t) + \ln(|\epsilon_y(t)|).$$

If one assumes that the noises  $\epsilon_x$  and  $\epsilon_y$  are independent Gaussian white noises, then thanks to the fact that  $\text{var}[\ln(|\epsilon|)] \approx 1.23$ , one can compute the correlation coefficient of  $\Omega_x$  and  $\Omega_y$  from the correlation of  $\omega_x$  and  $\omega_y$ . The obtained results for all data series are summarized in Table II. One clearly sees that the correlation coefficient of magnitude processes is for all series close to 20% while the estimated coefficients for the  $\Omega$  components are close to 1.<sup>2</sup> This result strongly suggests that the processes  $\Omega_x$  and  $\Omega_y$  are identical and therefore  $\Omega$  is a scalar quantity. One thus has (up to season components)

$$\delta_\tau v_x(t) = e^{\Omega_\tau(t)} \epsilon_x(t),$$

$$\delta_\tau v_y(t) = e^{\Omega_\tau(t)} \epsilon_y(t).$$

The scalar  $e^{\Omega_\tau(t)}$  is simply the (stochastic) amplitude of velocity fluctuation vector at scale  $\tau$ .

<sup>2</sup>Notice that estimated coefficients greater than 1 are probably due to our hypothesis concerning the normality of  $\epsilon_{x,y}$ ; such an assumption can only be a rough approximation for some series because of finite-size and granularity effects.

TABLE II. Correlation coefficients of magnitude components for the different sites.

Location	$\omega$ correlations	$\Omega$ correlations
Vignola (Ajaccio)	0.19	1.16
Ajaccio	0.22	1.31
Bastia	0.20	1.10
Calvi	0.14	1.10
Conca	0.22	1.07
Figari	0.17	1.32
Renno	0.21	0.71
Sampolo	0.11	0.68
Eindhoven	0.22	1.01
I. J. Muiden	0.22	0.99
Schiphol	0.21	0.98

According to these findings, in the following we compute a surrogate of the scalar process  $\Omega(t)$  as follows:

$$\omega_\tau(t) = \frac{1}{2} \ln[\delta_\tau v_x(t)^2 + \delta_\tau v_y(t)^2], \quad (31)$$

which is less noisy than individual magnitudes  $\omega_x$  or  $\omega_y$ . Let us notice, as already mentioned, that if one replaces in previous analysis  $\delta_\tau v_{x,y}$  with the error term in a Langevin model of  $v_{x,y}$  as in Eq. (30) or by small-scale wavelet coefficients, all the results remain unchanged [48]. Since the results presented below do not depend on the chosen small scale  $\tau$  (we focused on properties involving mainly lags greater than  $\tau$ ), we omit any reference to this scale and denote  $\omega(t)$  the local “magnitude” estimated at small scale according to Eq. (31).

The process  $\omega(t)$  also possesses a seasonal component which means that seasonal effects manifest not only through an additive (locally) periodic component but also through a diurnal modulation of the velocity stochastic amplitude. This multiplicative seasonal component has been estimated using the same local least-squared method as for the additive components [48]. In the following, we assume that all seasonal effects have been removed from the estimated field  $\omega(t)$ .

Along the line of the method described in Sec. II C, we have estimated the magnitude  $\omega(t)$  correlation functions  $\rho(\Delta t) = \text{cov}[\omega(t), \omega(t + \Delta t)]$  for all the time series. As illustrated in Fig. 6, when one plots  $\rho^{1/2}(\Delta t)$  as a function of  $\ln(\Delta t)$  one observes, for all series, a decreasing linear function that becomes zero above some lag  $T$  (notice that, because of the arbitrary shift we made for presentation purpose in Fig. 6, the zero value of correlations corresponds, for each graph, to the value of the plateau observed at large lags). It is striking to observe that all slopes are close to each other and that the “correlation” scale (integral scale) is roughly the same for all sites. In order to handle less noisy curves, we have plotted in Fig. 7(b), within the same representation, the mean correlation function over all sites in Corsica, over all sites in Netherlands and for the high-frequency series at Vignola [in Fig. 7(a) the same graphs are displayed using a linear representation]. Up to some remaining bump around the lag of 1 day due to the nonperfect removing of the sea-

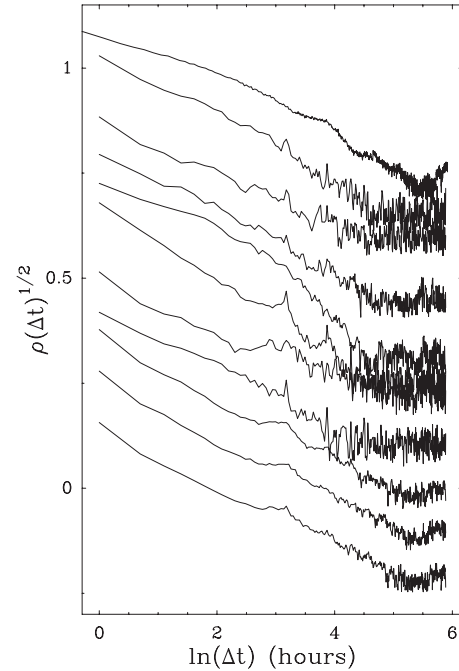


FIG. 6. Square root of magnitude covariance functions estimated for all wind series (additive and multiplicative seasonal components have been removed). The three bottom graphs correspond to Netherlands hourly series while the top graph is correlation of magnitudes associated with the “high-frequency” Vignola data series. All the graphs have been arbitrary shifted vertically for clarity purpose. One can observe comparable values of the parameters  $\beta^2$  and  $T$  (see text).

sonal components, one observes a well defined linear dependence on a range  $[\ln(\tau), \ln(T)]$ . This means that for all wind series, the covariance of  $\omega(t)$  reads ( $\Delta t > \tau$ )

$$\rho(\Delta t) = \beta^2 \ln^2\left(\frac{T}{\Delta t}\right).$$

In Sec. II D, we have explained how such a square logarithmic dependence of the single point covariance can be the result of logarithmic-correlated Eulerian and Lagrangian fields. This feature has also been observed on various labo-

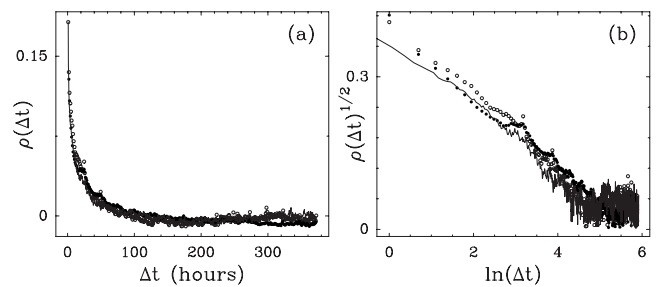


FIG. 7. Mean magnitude correlation functions associated with wind series in Corsica (○) and Netherlands (●) (all seasonalities have been removed). The solid line represents the magnitude covariance of the Vignola series (10 min rate). (a) The graphs are in linear scales. (b) The square root of the covariances are represented as function of the logarithm of the time lag  $\Delta t$ .

ratory turbulence data [12,38]. These observations are therefore direct evidences that a random cascade mechanism can be involved in the energy transfer at scales much greater than the usual turbulent microscale. Let us remark that the value of the integral scale we found is  $T \approx 5$  days in Holland and Corsica and the value of the slope  $\beta \approx 0.07$ . In order to deduce Eulerian (or Lagrangian) value of the intermittency coefficients, one would need to know the value of  $\frac{T}{\eta}$ , where  $\eta$  is a small time scale cutoff above, which Lagrangian variations are no longer intermittent. For example, if one sets  $T \approx 5$  days and one chooses  $\eta$  to be a typical time scale separating microscale and mesoscale, i.e.,  $\eta \approx 10$  min, according to Eq. (28) one gets an Eulerian intermittency coefficient  $\lambda^2 \approx 0.03$ , i.e., very close to the value found for fully developed turbulence (see, e.g., [12,19,20]).

#### IV. CONCLUSION AND PROSPECTS

The goal of this paper was to provide evidences that the surface-layer wind fluctuation statistics in the mesoscale to large-scale range are, very much like microscale turbulent statistics, characterized by strongly intermittent properties. We have first reviewed how the intermittency of continuous random cascades can be advantageously studied using magnitude correlation analysis as compared to standard scaling or magnitude cumulant estimations. Within this framework and using various wind velocity and direction time series in Corsica (France) and Netherlands, we have shown that one can define a scalar magnitude field that displays universal squared logarithmic correlation functions. Such a peculiar shape of time correlation functions at a fixed position is shown to result from a continuous cascade (with logarithmic-correlated magnitude) that governs the fluctuations in both Eulerian and Lagrangian frames. The same behavior has been observed in laboratory turbulence experiments. The existence of some mesoscale “energy cascade” and other similarities with the 3D isotropic turbulence properties raises various fundamental questions. Unlike synoptic circulations, mesoscale motions can be associated with a wide variety of phenomena covering a large range of characteristic scales from thunderstorms, mountain waves to front dynamics. In that respect, the universal features discussed in this paper have to be confirmed using further experimental data. Let us note however that a characteristic time scale of few days is usually associated with front dynamics [2] and some comparable typical time scales have been already reported in the literature [5,7]. From a practical point of view our findings lead to a better characterization of the statistical properties of wind fluctuations. The framework of intermittent statistics and random cascade models can be applied to address problems related to wind resources assessing, extreme events characterization or to design a simple stochastic model in order to perform short-term wind predictions [48,51].

#### ACKNOWLEDGMENTS

We acknowledge “Royal Netherlands Meteorological Institute” [40] for the availability of the potential wind speed data in Netherlands and B. Chabaud and B. Castaing for the

permission to use their experimental turbulence data. We also thank an anonymous referee for helpful remarks and suggestions.

#### APPENDIX: ERRORS IN INTERMITTENCY COEFFICIENT ESTIMATION

In this appendix, we provide some auxiliary computations related to the discussion on errors in the estimates of  $\lambda^2$  of Sec. II C. The estimation relies upon Eq. (14) and one can either performs a regression of the variance of  $\omega_\tau$  as a function of  $\ln(\tau)$  according to Eq. (8) (method I) or, according to Eq. (12), a fit of the estimated covariance of  $\omega_\tau$  (at fixed  $\tau$ ) as a function of the logarithm of the lag (method II). Let  $\mathcal{E}_I^2$  and  $\mathcal{E}_{II}^2$  be the square estimation errors of  $\lambda^2$  when using, respectively, methods I and II. We will denote by  $\mathcal{E}_{I,\Omega}^2$  (respectively,  $\mathcal{E}_{II,\Omega}^2$ ) the square error associated with the  $\Omega_\tau$  term in Eq. (14) with method I (respectively, method II) and by  $\mathcal{E}_{I,\varepsilon}^2$  (respectively,  $\mathcal{E}_{II,\varepsilon}^2$ ) the square error related to the noise term  $\ln(|\varepsilon|)$  with method I (respectively, method II). We have, obviously,

$$\mathcal{E}^2 = \mathcal{E}_\Omega^2 + \mathcal{E}_\varepsilon^2. \quad (\text{A1})$$

Each error is related to the estimation of the slope of a linear regression of  $V_k$  as a function of  $l_k$ , where  $V_k$  can be, according to method I or II, the variance or covariance of  $\omega_\tau$  and  $l_k$  is the logarithm of scale  $\tau$  or the logarithm of the lag. Consistently with previous notations,  $e_{I,\Omega}^2$  and  $e_{I,\varepsilon}^2$  (respectively,  $e_{II,\Omega}^2$  and  $e_{II,\varepsilon}^2$ ) stand for the square errors in the determination of  $V_k$ 's with method I (respectively, method II) associated with first and second terms in Eq. (14). If one assumes that these errors do not depend on  $k$  (this assumption is not true but one can consider the maximum error value over all  $V_k$  in order to get an upper bound of the final error) and if  $D_f$  denotes by  $N_f$  the number of points used in the fit and by  $D_l$  the mean-square variation of  $l_k$ 's, we have (whatever are the subscripts)

$$\mathcal{E}^2 = \frac{e^2}{N_f D_l}. \quad (\text{A2})$$

For the sake of simplicity and since we only want a rough estimation of the errors, we suppose that, in both methods, the fit is performed over a domain of order of the integral scale  $T$ , so that  $D_l \sim (\ln T)^2$ . We also choose uniformly sampled  $l_k$  values, i.e.,  $N_f \sim \ln T$ . The former linear regression error becomes

$$\mathcal{E}^2 \approx \frac{e^2}{(\ln T)^3}. \quad (\text{A3})$$

It then remains to compute the error terms  $e_{I,II}^2$  associated with the estimation of  $V_k$ 's. Since  $\Omega_\tau$  is a Gaussian process with a slowly decaying covariance, the estimation error of the variance or the covariance of  $\Omega_\tau$  is of the same magnitude order (i.e.,  $e_{I,\Omega}^2 \approx e_{II,\Omega}^2$ ) and is proportional to mean square deviation of  $\Omega_\tau^2$  [ $\sim \lambda^4 (\ln T)^2$ ] divided by the number of independent samples in the signal. If  $N$  is the overall sample size, for a correlated process of correlation function  $\rho(i)$ , the effective number of independent data is [52]

$$N^* = \left[ N^{-1} + \frac{2}{N^2} \sum_{i=1}^N (N-i)\rho(i) \right]^{-1}. \quad (\text{A4})$$

Since, for the process  $\Omega_\tau$ ,  $\rho(i)=\ln(T/i)$  if  $i \leq T$  [ $\rho(i)=0$ , otherwise] it turns out after a little algebra that for  $N \gg T \gg 1$ , we have

$$N^* \simeq \frac{N}{2T \ln T}, \quad (\text{A5})$$

which leads finally to

$$e_{I,\Omega}^2 \simeq e_{II,\Omega}^2 \sim \frac{2T\lambda^4 \ln(T)^3}{N}. \quad (\text{A6})$$

The value of  $e_\varepsilon^2$  depends on the method one considers. In method I, this error is related to the variance of  $[\ln(|\varepsilon|)]^2$  at the scale  $\tau=T$  which is roughly

$$e_{I,\varepsilon}^2 \simeq \frac{T \text{var}[\ln(|\varepsilon|)^2]}{N} \sim \frac{16.5T}{N}, \quad (\text{A7})$$

while the error according to method II only involves the scale  $\tau=1$  and, since  $\varepsilon$  is a white noise, is proportional to the variance of  $\ln(|\varepsilon|)$ ,

$$e_{II,\varepsilon}^2 \simeq \frac{\text{var}[\ln(|\varepsilon|)]}{N} \simeq \frac{1.2}{N}. \quad (\text{A8})$$

If one summarizes our findings, we see that the estimation error of method I is

$$\mathcal{E}_I^2 \simeq \frac{2T\lambda^4}{N} + \frac{16.5T}{N(\ln T)^3}, \quad (\text{A9})$$

while the error associated with method II is

$$\mathcal{E}_{II}^2 \simeq \frac{2T\lambda^4}{N} + \frac{1.2}{N(\ln T)^3}. \quad (\text{A10})$$

- 
- [1] U. Frisch, *Turbulence* (Cambridge University Press, Cambridge, England, 1995).
- [2] J. Holton, *An Introduction to Dynamic Meteorology* (Elsevier Academic, Burlington, 2004).
- [3] M. K. Lauren, M. Menabde, A. W. Seed, and G. Austin, *Boundary-Layer Meteorol.* **90**, 21 (1999).
- [4] S. Lovejoy, D. Schertzer, and J. D. Stanway, *Phys. Rev. Lett.* **86**, 5200 (2001).
- [5] V. Gupta and E. Waymire, *J. Geophys. Res.* **95**, 1999 (1990).
- [6] V. Gupta and E. Waymire, *J. Appl. Meteorol.* **32**, 251 (1993).
- [7] R. G. Kavasseri and R. Nagarajan, *IEEE Trans. Circuits Syst., I: Regul. Pap.* **51**, 2255 (2004).
- [8] F. Botcher, S. Barth, and J. Peinke, *Stochastic Environ. Res. Risk Assess.* **21**, 299 (2006).
- [9] M. Kholmyansky, L. Moriconi, and A. Tsinober, *Phys. Rev. E* **76**, 026307 (2007).
- [10] A. Arneodo, J. F. Muzy, and D. Sornette, *Eur. Phys. J. B* **2**, 277 (1998).
- [11] J. F. Muzy, J. Delour, and E. Bacry, *Eur. Phys. J. B* **17**, 537 (2000).
- [12] J. Delour, J. F. Muzy, and A. Arneodo, *Eur. Phys. J. B* **23**, 243 (2001).
- [13] E. Bacry, A. Kozhemyak, and J. F. Muzy, *J. Econ. Dyn. Control* **32**, 156 (2008).
- [14] A. Kozhemyak, Ph.D. thesis, Ecole Polytechnique, 2006.
- [15] J. Delour, Ph.D. thesis, Université de Bordeaux I, 2001.
- [16] F. Anselmet, R. Antonia, and L. Danaïla, *Planet. Space Sci.* **49**, 1177 (2001).
- [17] B. Lashermes, P. Abry, and P. Chainais, *Int. J. Wavelets, Multiresolut. Inf. Process.* **2**, 497 (2004).
- [18] J. F. Muzy, E. Bacry, R. Baile, and P. Poggi, *EPL* **82**, 60007 (2008).
- [19] S. Basu, E. Foufoula-Georgiou, B. Lashermes, and A. Arneodo, *Phys. Fluids* **19**, 115102 (2007).
- [20] A. Arneodo, S. Manneville, and J. F. Muzy, *Eur. Phys. J. B* **1**, 129 (1998).
- [21] B. Castaing, Y. Gagne, and E. Hopfinger, *Physica D* **46**, 177 (1990).
- [22] J. F. Muzy and E. Bacry, *Phys. Rev. E* **66**, 056121 (2002).
- [23] E. Bacry and J. F. Muzy, *Commun. Math. Phys.* **236**, 449 (2003).
- [24] B. B. Mandelbrot, *J. Fluid Mech.* **62**, 331 (1974).
- [25] B. B. Mandelbrot, *C.R. Seances Acad. Sci., Ser. A* **278**, 289 (1974).
- [26] B. B. Mandelbrot, *J. Stat. Phys.* **110**, 739 (2003).
- [27] J. P. Kahane and J. Peyrière, *Adv. Math.* **22**, 131 (1976).
- [28] Y. Guivarc'h, *C. R. Acad. Sci., Ser. I: Math.* **305**, 139 (1987).
- [29] G. M. Molchan, *Commun. Math. Phys.* **179**, 681 (1996).
- [30] G. M. Molchan, *Phys. Fluids* **9**, 2387 (1997).
- [31] Q. Liu, *Asian J. Math.* **6**, 145 (2002).
- [32] F. Schmitt and D. Marsan, *Eur. Phys. J. B* **20**, 3 (2001).
- [33] J. Barral and B. B. Mandelbrot, *Probab. Theory Relat. Fields* **124**, 409 (2002).
- [34] P. Chainais, R. Riedi, and P. Abry, *IEEE Trans. Inf. Theory* **51**, 1063 (2005).
- [35] A. Arneodo, E. Bacry, S. Manneville, and J. F. Muzy, *Phys. Rev. Lett.* **80**, 708 (1998).
- [36] E. Bacry, A. Kozhemyak, and J. F. Muzy, *Quant. Finance* (to be published).
- [37] L. Chevillard, S. G. Roux, E. Leveque, N. Mordant, J. F. Pinton, and A. Arneodo, *Phys. Rev. Lett.* **95**, 064501 (2005).
- [38] B. Castaing, *Eur. Phys. J. B* **29**, 357 (2002).
- [39] B. Castaing, *Phys. Rev. E* **73**, 068301 (2006).
- [40] See [www.knmi.nl/samenw/hydra/index.html](http://www.knmi.nl/samenw/hydra/index.html)
- [41] I. Van der Hoven, *J. Meteorol.* **14**, 160 (1957).
- [42] A. H. Oort and A. Taylor, *Mon. Weather Rev.* **97**, 623 (1969).
- [43] G. Nastrom, K. Gage, and W. Jasperson, *Nature (London)* **310**, 36 (1983).
- [44] D. Lilly, *J. Atmos. Sci.* **40**, 749 (1983).
- [45] J. Kaimal, *J. Atmos. Sci.* **35**, 18 (1978).
- [46] M. Taqqu and G. Samorodnisky, *Stable Non-Gaussian Random Processes* (Chapman & Hall, New York, 1994).

- [47] B. Abraham and J. Ledolter, *Statistical Methods for Forecasting* (Wiley, New York, 1983).
- [48] R. Baile, J. F. Muzy, and P. Poggi (unpublished).
- [49] M. K. Lauren, M. Menabde, and L. Austin, *Boundary-Layer Meteorol.* **100**, 263 (2001).
- [50] O. Chanal, B. Chabaud, B. Castaing, and B. Hebral, *Eur. Phys. J. B* **17**, 309 (2000).
- [51] R. Baile, J. F. Muzy, and P. Poggi, Proceedings of World Renewable Energy Congress, Bangkok, Thailand, 2009 (to be published).
- [52] G. V. Bayley and J. M. Hammersley, *J. R. Stat. Soc.* **8**, 184 (1946).